Explosive welding of stainless steel–carbon steel coaxial pipes

Ehsan Zamani · Gholam Hossien Liaghat

Abstract Bi-metallic corrosion resistant steel pipes were produced through explosive welding process. The weldability window of the stainless steel pipe (inner pipe) and the carbon steel pipe (outer pipe) was determined by the use of available semi-empirical relations. The impact velocity of the pipes as the most important collision parameter was calculated by the finite element simulation. Direct effect of the explosive mass reduction on the bonding interface of the pipes was studied. Optical microscopy study showed that a transition from a wavy interface to a smooth one occurs with decrease in explosive load.

Introduction

Explosive welding is an unconventional technique of joining two or more metals by the use of controlled explosive detonation. This is a solid phase process, in which the bonding is produced by the high velocity oblique collision between the metals to be welded. As the detonation is initiated, the flyer metal (plate or pipe) is drastically accelerated by the pressure of detonation and flies with very high velocity towards the parent metal (plate or pipe) as shown in Fig. 1. The stand-off provides the distance across which the flyer metal can be accelerated and reached the necessary impact velocity at which a metallurgical bond is formed between the metal components [1]. The surface oxide films are detrimental to the establishment of the bond. These films are swept away from the

interface by a high velocity jet produced at the collision point of metals. The metal components are then cleaned of any surface film by the jet action. At the collision point, virginally clean surfaces are brought together under very high pressure. The pressure has to be sufficiently high and for a sufficient length of time to achieve inter-atomic bonds [2, 3]. The bond is metallurgical in nature and usually is stronger than the weaker of the mating metals [3, 4].

One of the interesting characteristics of explosive welding is that a wavy bond is formed along the mating surface after the event [5]. This bond has generally a good strength because of the large and wavy contact surface, although a straight interface can be at least equality strong as the one exhibiting a wavy interface [6].

While the process can be used to weld similar materials, its major industrial potential lies in the fact that it can be used to join dissimilar metals, many of which are impossible to join by conventional methods (e.g., because of dramatically different melting points) [8]. Also, the process can clad one or more different metal layers onto either, or both faces of a parent metal, simultaneously [9]. Furthermore, the process is capable of joining with higher surface areas due to its ability to distribute the high energy density through explosion [10].

There is a considerable demand for cladded plates and pipes in both chemical and nuclear industries. As low carbon steel has low corrosion resistance, therefore, it maybe cladded with the materials such as aluminum, titanium, and stainless steel that can be suitable for using in corrosive environment. The cladding of steel with a corrosion resistant overlay has a number of advantages. It is economic, since, clad is cheaper than solid stainless steel. Also, it minimizes the risk of catastrophic failure due, for example, to stress corrosion cracking. Hence, it provides the optimum combination of mechanical properties with corrosion resistance [11].

E. Zamani · G. H. Liaghat (✉)
Department of Mechanical Engineering, Impact Mechanics
and Explosion Lab, Tarbiat Modares University,
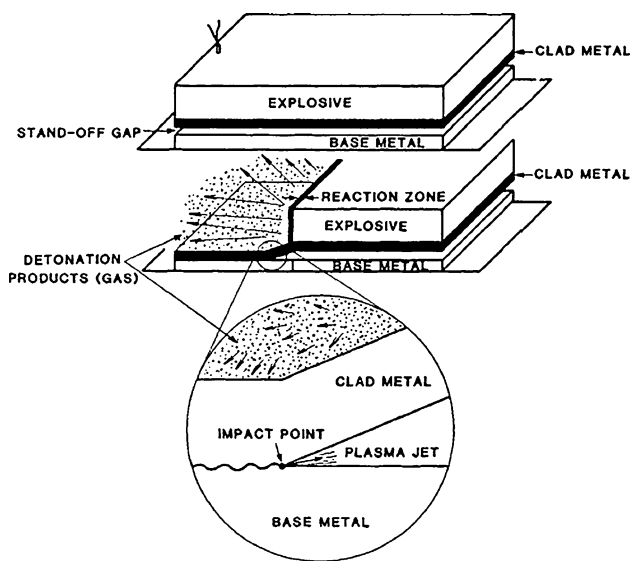P.O. Box: 14115-143, Tehran, I.R. Iran
e-mail: ghlia530@modares.ac.ir

Fig. 1 Explosive welding process in planar geometry [7]

Some relatively new articles concerned with the explosive welding of steel plates are available. Explosive welding parameters of chemically identical flat steel plates and their effects on microstructure, microhardness, and tensile-shear strength in original and heat-treated samples were investigated by Acarer et al. [12, 13]. It was shown that the bonding interface changed from a straight to a wavy structure when the explosive loading and stand-off distance were increased. For wavy interfaces, when the explosive loading was increased, the wavelength and amplitude increased.

In addition, Kacar and Acarer reported on the explosive cladding of 2205 grade duplex stainless steel-DIN-P355GH grade vessel steel [14] and 316L stainless steel-DIN-P355GH grade vessel steel [15]. Microstructure, hardness, tensile-shear strength, and fracture toughness of the cladded plates were evaluated. They showed that the mechanical properties of the low carbon steels can be increased by explosive cladding with duplex and austenitic stainless steels.

The authors know of only four main references concerned with the explosive cladding of cylindrical members. First, Carlson and Simons [16] joined 0.02–0.05 inch wall zircaloy tubes to 6.0 inch o.d. × 1.3 inch wall stainless steel, using Metabel and spiraled Primacord charges. In an evacuated environment jetting seemed not to have occurred, but the bond was reasonable. It probably depended to a great extent on the degree of vacuum and on the standard of cleanliness of the impinging surfaces. Second, Segel [17] attempted to clad inside of 3.6–3.75 inch o.d. × 0.17–0.25 inch wall zircaloy tubes with 0.015–0.12 inch thick aluminum. Experiments employing a simultaneous detonation of charges inside and outside the specimens failed; others using large external dies

of steel were partially successful and the resulting bonds were similar to those of [16]. Third, Willis and Murdie [18] joined the ends of 3.24 inch o.d. × 0.12 inch wall aluminum tubes by explosively welding them to a concentric 3.5 inch o.d. × 0.12 inch wall aluminum sleeve supported by a heavy steel die. The charge used was a double layer of Cordtex wound in a tight helix and separated from the work pieces by a fiber-reinforced rubber lining. The performance of the joint was good. The authors reported that the interface was not continuous and that joining may have been by "a series of scattered microwelds". Fourth, Dalrymple and Johnson [19] described the experiments in which the internal surface of 2.0 inch o.d. × 0.125 inch wall steel tubes were explosively clad with 0.062 inch thick copper, and the bonds evaluated. Jetting occurred using Cordtex charges and the bond shear strength exceeded that of the copper.

The study reported below was focused on the explosive welding of a bi-metallic pipe, in which the outer and the inner pipes were CK22 carbon steel and 316L stainless steel, respectively. This article presents a relatively complete research on the explosive welding in the cylindrical geometry. In the first part, the weldability window of two metals was developed using the available semi-empirical relations. This window enables the establishments of analytical conditions for the formations of wavy and smooth bond interfaces.

In the second part of the study, bi-metallic pipes were manufactured successfully. The experiments were conducted to consider the effects of variation of explosive loading on the bonding quality using the optical microscope. The velocity that the flyer pipe impacts the parent pipe was calculated by the finite element simulation. This parameter is used to determine the coordinates of the point associated to each experiment on the weldability window.

Analysis

In both planar and cylindrical geometries of explosive welding, the basic welding parameters can be summarized as: the impact velocity (V_p), the collision point velocity or welding velocity (V_w), and the dynamic angle of collision (β) [20]. The process variables that affect these parameters are explosive detonation velocity, explosive load, stand-off distance and/or initial angle of flyer metal in the inclined set-up [3, 21, 22].

Each welding parameter has critical boundaries which passing beyond them may cause some defects in the weld zone or even lead to failure of metals junction. For example, if (V_w) reaches a supersonic value, there is no jetting. The same event happens if the value of the collision

Fig. 2 a Mechanism of parallel configuration explosive welding. b Velocity diagram [25]
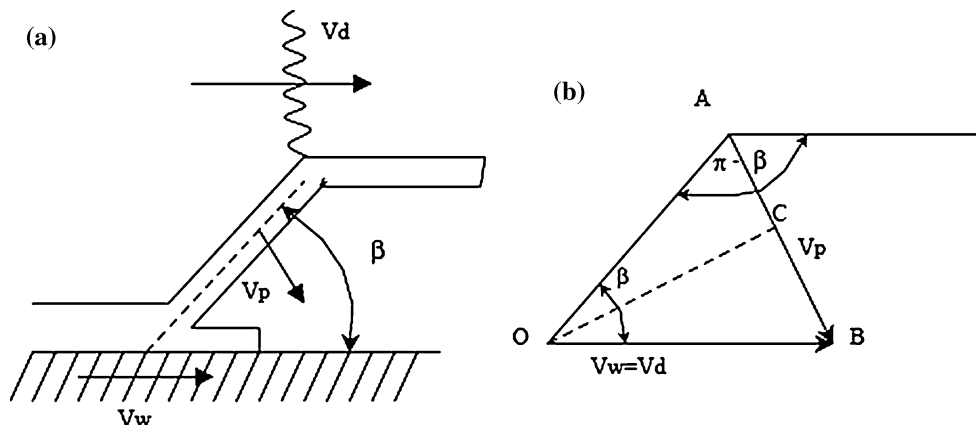
angle is less than its minimum limit. Nouri [23] has suggested the appropriate value of (β) as $5° < \beta < 25°$.

The collision angle can be calculated from the collision point and the impact velocities by simple geometrical considerations. A suggested geometrical analysis shows that the impact velocity bisects the angle between the initial plate (or pipe) and the deformed plate (or pipe) orientations [24, 25].

Figure 2 shows the above parameters on a velocity diagram. According to this diagram, a kinematical relation can be written as (triangle OAB is isosceles):

$$V_p/2 = V_w \sin(\beta/2) \tag{1}$$

Wittman [26] and Deribas et al. [27] developed an explosive weldability window (Fig. 3), in which the collision angle (β) is plotted in the ordinates and the welding velocity (V_w), is plotted in the abscissa. They studied jet formation, the critical impact pressure, the maximum impact velocity, and wavy–smooth transition velocity.

Equation 2 gives the lower limit of the weldability window, where β is in radians, k_1 is a constant, H is the Vickers hardness in N/m², and ρ is the density in kg/m³ [28]:

$$\beta = k_1 \left(\frac{H}{\rho V_w^2}\right)^{\frac{1}{2}} \tag{2}$$

The value of k_1 is 0.6 for high-quality pre-cleaning of surfaces and 1.2 for imperfectly cleaned surfaces.

Equation 3 gives the upper limit of the weldability window [27, 28]:

$$\text{Sin } \frac{\beta}{2} = \frac{k_2}{t_f^{0.25} V_w^{1.25}} \tag{3}$$

where, t_f represents the thickness of flyer metal and $k_2 = \sqrt{E/(12\,\rho\,(1-2\upsilon))}$, in which E is the Young's module in N/mm² and υ is the Poisson's ratio of the metal.

Analyses of Cowan and Holtzman [29] and Cowan et al. [30] give an expression for the minimum transition velocity, above which a wavy interface is obtained. They
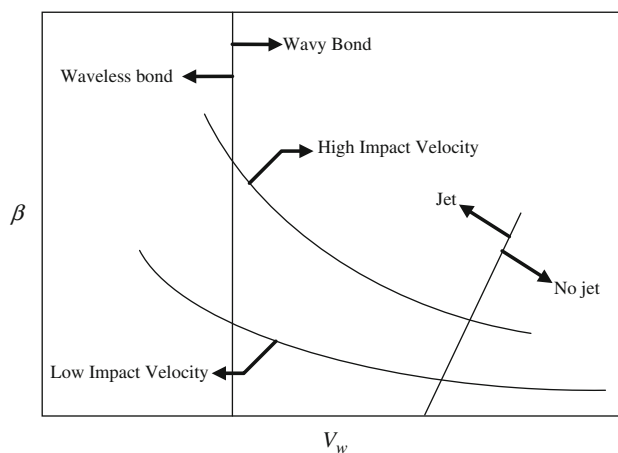

Fig. 3 Theoretical and practical weldability window [26]

introduced the following Reynolds number for the smooth–wavy transition that gives the left boundary of the window:

$$\text{Re} = \frac{(\rho_f + \rho_p)\,V_w^2}{2\,(H_f + H_p)} \tag{4}$$

where, the subscripts f and p represent the flyer and parent metals, respectively. In all of Cowan's experiments, Eq. 4 in which R_e is equal to 10.6 describes the transition very well. The limitation is that he studied only one collision angle, $\beta = 12°$ [25]. Therefore, it is necessary to obtain a relationship between the Reynolds number and the collision angle. Jaramillo et al. [31] developed a model for the three material couples, i.e., Fe–Fe, Cu–Cu and Al–Al. They obtained the following general relationship between the Reynolds number and the collision angle with a correlation factor = 0.9853:

$$\text{Re} = 93.02(\pm9.62) - 13.45(\pm2.06)\beta + 0.71(\pm0.14)\beta^2$$
$$- 0.012(\pm0.03)\beta^3 \tag{5}$$

which provides a very good approximation of the smooth–wavy transition boundary.
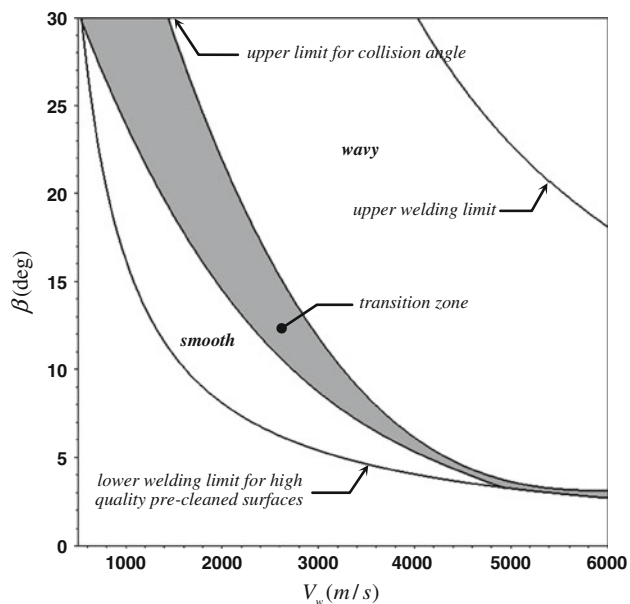
Fig. 4 Weldability window of 316L stainless steel and CK22 carbon steel pipes

Figure 4 shows the application of Eqs. 1–5 to the V_w vs. β. The smooth-wavy interface transition is shown in this plot and two regions are clearly distinguished. It can be seen that the broadness of the transition zone decreases as the explosive velocity increases.

Experimental procedure

Pipes and anvil

Figure 5a shows the prepared pipes divided into 100 mm length pieces. From the right to the left, they are thin and thick-walled stainless steel pipes (as the flyer pipes) and carbon steel pipes (as the parent pipes), respectively. The steel anvil manufactured to protect the outer geometry of the parent and the final duplex pipes are also shown in Fig. 5b. It was made from 1.2713 grade steel, which exhibits excellent resistance to impact loads. Table 1 summarizes the geometrical dimensions of the pipes.

Set-up

All colliding surfaces of the pipes were completely ground and polished to 1 μm finish. The flyer pipe was concentrically fitted in the parent pipe as schematically shown in Fig. 6a. Backer anvil surrounded the external pipe and finally, the internal space of the flyer pipe was filled with the TNT powder with the density of 1 gr/cm³. A detonator started the process.

Explosive mass reducers

The effects of charge mass reduction on the quality of the bond were investigated additionally. Mass reduction of the explosive was performed through application of some sacrificial inserts located at the centerline of the flyer pipes. Each insert which can be made from wood, plastic or similar worthless materials, occupies some part of the flyer's internal volume and therefore, decreases the mass of required explosive charge (Fig. 7).

In addition to the described boundaries shown in Fig. 3, the lower and the upper limits of the dynamic angle of collision are experimentally determined by Bahrani and Crossland [32]. A lower limit of 2–3° and upper limit of 31° have been suggested and the data published are in general agreement with these values.

In the present research, the weldability window was plotted for CK22 carbon steel and 316L stainless steel seamless pipes, separately. Then the first plot was superimposed on the other one. The overlapped area represented the working range of the parameters applicable to the combination of two metals. The required parameters for the pipes are $H_v = 177$ kg/mm², $E = 193$ GPa, and $\rho = 7830$ kg/m³ for 316L stainless steel pipe and $H_v = 153$ kg/mm², $E = 200$ GPa, and $\rho = 7800$ kg/m³ for CK22 carbon steel pipe, all were obtained by standard mechanical tests. The determined weldability window of carbon steel and stainless steel pipes is shown in Fig. 4.

Fig. 5 a Carbon steel and stainless steel pipes. **b** Backer anvil

Table 1 Dimensions of the pipes

	Inside diameter (mm)	Outside diameter (mm)	Wall thickness (mm)
Stainless steel 316L (SCH. 5)	30.1	33.4	1.65
Stainless steel 316L (SCH. 40)	26.64	33.4	3.38
Carbon steel CK22	38	50	6

A ream of inserts was made for each type of the flyer pipes, with their specifications given in Table 2. In this table, d and m_e represent the diameter of each insert and its associated explosive mass that fills the flyer, respectively.

Outcomes

All of the experiments with different parameters gave successful bonding. Figure 8 shows a bi-metallic pipe divided into some pieces. Monotonous expansion of the flyer pipe and its joining to the parent pipe are seen. Better judgment will be carried out by exploration of the interface optical images in the section of results and discussion.

Finite element simulation

Detonation velocity of the explosive used was equal to 5100 m/s. This velocity can be considered as the input value of the weldability window (Fig. 4). Therefore, the points associated to the experiments done, are located on the vertical line $V_d = 5100$ m/s. The ordinate of every point can be obtained from direct calculation of (β) if possible or via Eq. 1 if (V_P) is accessible. Since none of these parameters were available, the ordinates determination of interested points was the main obstacle to link between the welding window and the experiments results. This problem was disposed by numerical simulation described in the continuation.

Numerical simulations of the experiments were carried out using LS-DYNA software [33]. An axisymmetric

Fig. 7 Wooden inserts in different diameters

model of TNT filled stainless steel flyer and carbon steel parent pipes were developed. Surface to surface contact was defined between the explosive and flyer pipe and also between the flyer and parent pipes. Because of the axisymmetric consideration, the developed model appears as three rectangles, two of which, i.e., explosive and flyer pipe are in direct contact, while the flyer and parent pipes are spaced apart as equal as stand-off distance. The boundary conditions representing the existence of the backer anvil were included in the model. A detonator located at the first node of the centerline of explosive was also considered as the initial condition (Fig. 9).

Material model

The Johnson-Cook (J-C) material model (MAT_JOHNSON_COOK) was used for the pipes. Because of considering strain hardening effect, strain rate, and temperature, this model has attained very broad and successful usage in the simulation of dynamic and impact problems. The J-C model represents the flow stress with an equation of the form [34]:

$$\sigma = \left(A + B\,\bar{\varepsilon}_p^n\right)\left(1 + C\ln\dot{\varepsilon}^*\right)\left(1 - T^{*m}\right) \tag{6}$$

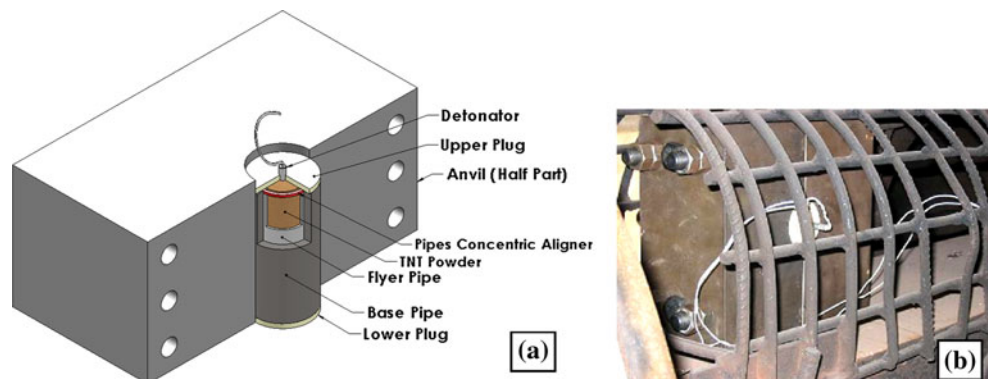**Fig. 6 a** Schematic view of the EWP package. **b** Assembled package in the explosion chamber

Table 2 Specifications of the inserts

Flyer SCH.5	d (mm)	8	12	16	20	22	24	26
Explosive capacity: 71 gr	m_e (gr)	66	60	51	40	33	26	18
	Weld achievement	Yes	Yes	Yes	Yes	No	No	No
Flyer SCH.40	d (mm)	4	8	10	13	16		
Explosive capacity: 56 gr	m_e (gr)	54	51	47	42	35		
	Weld achievement	Yes	Yes	No	No	No		

Fig. 8 A duplex pipe, divided into some parts

where,

$$\bar{\varepsilon}_p = \Sigma \dot{\bar{\varepsilon}}_p \, \Delta t \tag{7}$$

$$\dot{\varepsilon}^* = \dot{\bar{\varepsilon}}_p / \varepsilon_0, \quad (\varepsilon_0 = 1) \tag{8}$$

and

$$T^* = \frac{T - T_{room}}{T_{melt} - T_{room}} \tag{9}$$

Eqs. 7 and 8 represent the equivalent plastic strain and dimensionless equivalent strain rate, respectively. The five parameters A, B, C, m, n can be obtained for each material by mechanical tests. Table 3 shows the values of these parameters for the pipes [35, 36].

The high explosive material (MAT_HIGH_EXPLO-SIVE_BURN) was also used to model the explosive charge. For TNT with $\rho = 1$ gr/cm^3, the detonation velocity and the Chapman-Joguet (C-J) pressure were considered as $V_D = 5100$ m/s and $P_{CJ} = 7.5$ GPa, respectively [37].

Table 3 JC parameters of the pipes [35, 36]

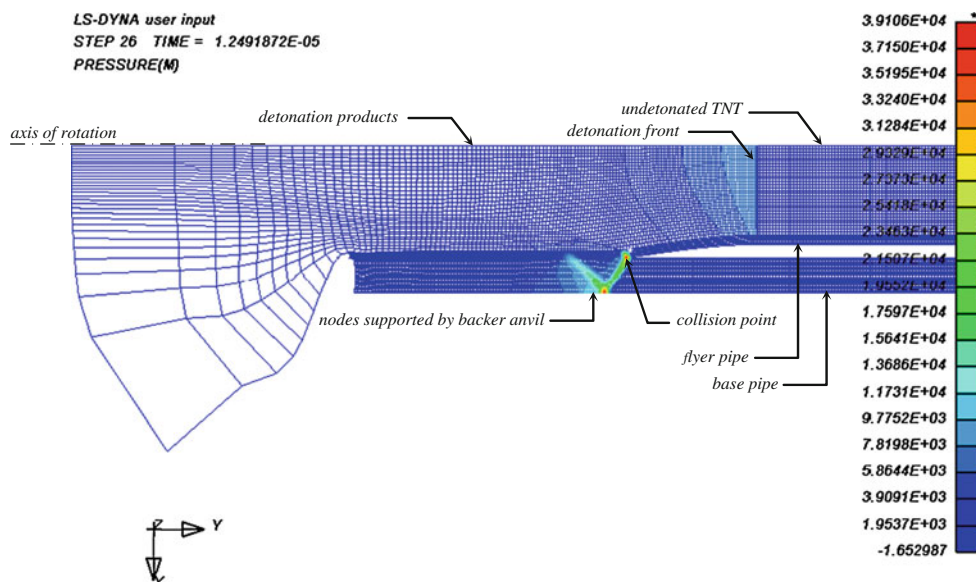|	A (MPa)	B (MPa)	C	m	n
Stainless steel (316L)	792	510	0.014	1.03	0.26
Carbon steel (CK22)	350	275	0.022	1.0	0.36

Fig. 9 Simulation of detonation, expansion of the flyer pipe and its collision to the parent pipe

Equation of state

As essential part of the numerical models used to simulate hydrodynamic and chemical reaction process is the equation of state (EOS) relating pressure, temperature, and density. The general form of an EOS can be demonstrated as

$$P = P(\rho, e) \tag{10}$$

where, e is the specific energy [37]. Among available equations, the Jones-Wilkins-Lee (JWL) and the Mie-Gruneisen equations of state were chosen for the explosive and the pipes, respectively. The JWL is perhaps the most popular EOS used in the high explosive community for a large class of problems [38]. The JWL EOS can be found to be used in the form [38, 39]:

$$P = A\left(1 - \frac{\omega}{R_1 V'}\right) e^{-R_1 V'} + B\left(1 - \frac{\omega}{R_2 V'}\right) e^{-R_2 V'} + \frac{\omega}{V'} E \tag{11}$$

where, $V' = \rho_0/\rho$ and $E = \rho_0 e$. A, B, R_1, R_2, and ω are constants of the explosive which satisfy the mass, momentum, and energy conservation equations.

The EOS most commonly used to describe inert solids is the Mie-Gruneisen equation [35]. It can be shown in the form [36]:

where, $\mu = \rho/\rho_0 - 1$ is the Gruneisen parameter, E is the reference of the metal's thermal energy and a, S_1, S_2, and S_3 are the material's constants [40].

Outcomes

Simulation was only done for the thin-walled flyer pipe (SCH. 5). For the flyer pipe filled with the explosive, the radial velocity diagrams of the middle nodes of the colliding surfaces are shown in Fig. 10. As shown, the velocity of the flyer pipe increases to 852 m/s and then drops rapidly. Collision occurs at this instant and the mentioned velocity is the impact velocity (V_P). Upon the occurrence of collision, the internal surface of the parent pipe starts to gain speed in the same direction with the flyer pipe. Both pipes gain the same velocity after 0.5 μs.

Results and discussion

Quality of joining

Optical micrographs of the bonded interfaces associated to the fully filled flyer pipes are shown in Fig. 11a, b. As seen, monotonously wavy interfaces and imperfection-free bonds

$$P = \rho_0 C^2 \mu \frac{[1 + (1 - \gamma_0/2)\mu - a/2\,\mu^2]}{[1 - (S_1 - 1)\mu - S_2\mu^2/(\mu+1) - S_3\mu^3/(\mu+1)^2]^2} + (\gamma_0 + a\mu)E \tag{12}$$

Fig. 10 Velocity diagrams of the middle nodes of colliding surfaces of the pipes, flyer pipe: SCH. 5
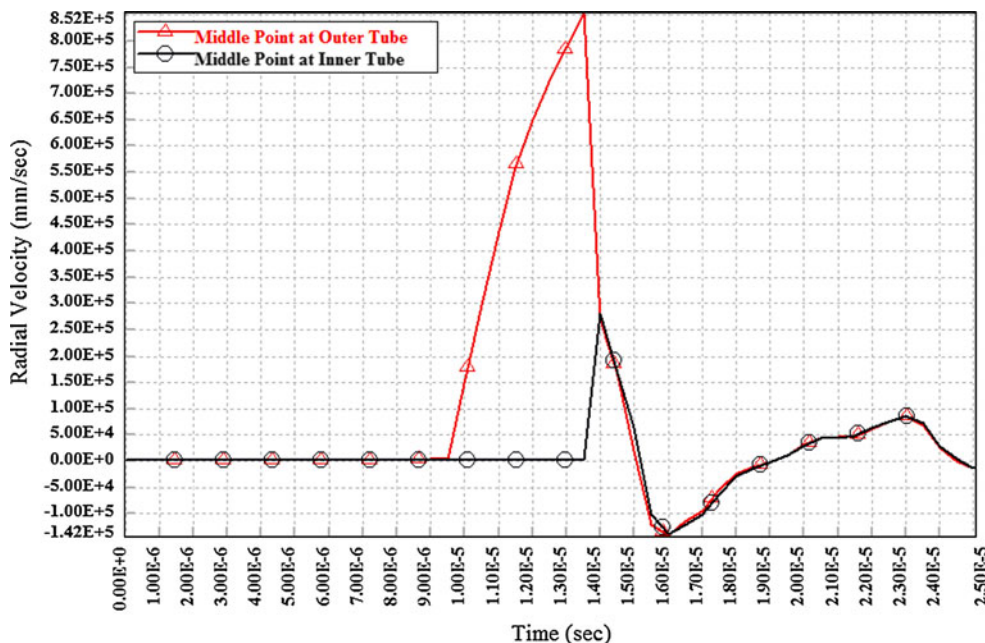
were obtained, which are the best evidences of the jet formation, fitness of collision parameters, and the positive effect of pre-cleaning of the colliding surfaces. Also, it appeared that the higher explosive loading of the flyer pipe in the left column (SCH. 5 flyer), compared with the right one (SCH. 40 flyer), caused larger amplitude and wavelength in the interface. Finally, it shall be asserted that both of these experiments were located in the wavy region of the weldability window (Fig. 4) and perfectly away from the transition zone, especially for the thin-walled flyer pipe.

According to the qualified bonding achieved and the maximum possible amount of the explosive used, it can be concluded that the welded interfaces have attained their maximum possible quality and strength. But a critical question for clad metals is "how good is the join"? To answer this question, one should note that the waviness (wavelength and amplitude) of interface increases with the increasing stand-off distance and/or explosive loading, for a constant collision point velocity. This effectively increases the bonding surface area of the metal components and produces a greater depth of shock hardening which in turn may lead to stronger joints [3, 41–43]. In addition, it is observed from the interface images that increasing the explosive loading would lead to a hook type locking mechanism. This mechanical locking can be clearly seen from the interface images in Fig. 11a. As a result, mechanical locking improves the bonding strength of the metals [42].

Optical micrographs in Fig. 12a–c show the effects of interface morphology with explosive loads. The least waviness is seen in Fig. 12c. As expected, joining strength became weaker with increasing of the inserts diameter. For the thin-walled flyer, wavy interface turned gradually into smooth interface up to the insert diameter of 20 mm and no joining was produced for larger diameters (Fig. 12a–c). But for the second series of flyer pipes and inserts, the situation was a little different. Here, approximate and complete smooth interfaces were produced for the 4 and 8 mm diameter inserts, respectively (Fig. 13a, b), and no bond was obtained for thicker inserts. Furthermore, some separations were seen along the interface in the latter image.

The high pressure shock waves that develop during the collision of pipes cause extensive plastic deformation at the contact region. Grains near the interface were generally elongated parallel to the detonation direction (shock hardened region). Elongation of the near-bond grains was also reported by previous researcher [3, 41].

Collision angle

Most of the experiments performed in this study were successful. Good bonding was achieved in all experiments except test shown in Fig. 13b. According to Eq. 1 and Fig. 10, the collision angle (β) can be calculated for the thin-walled fully filled flyer pipe (Fig. 11a) as

Fig. 11 Wavy welded interface of the pipes (*upper layer*: flyer pipe, *lower layer*: parent pipe), direction of the detonation front progress: from the *left* to the *right*
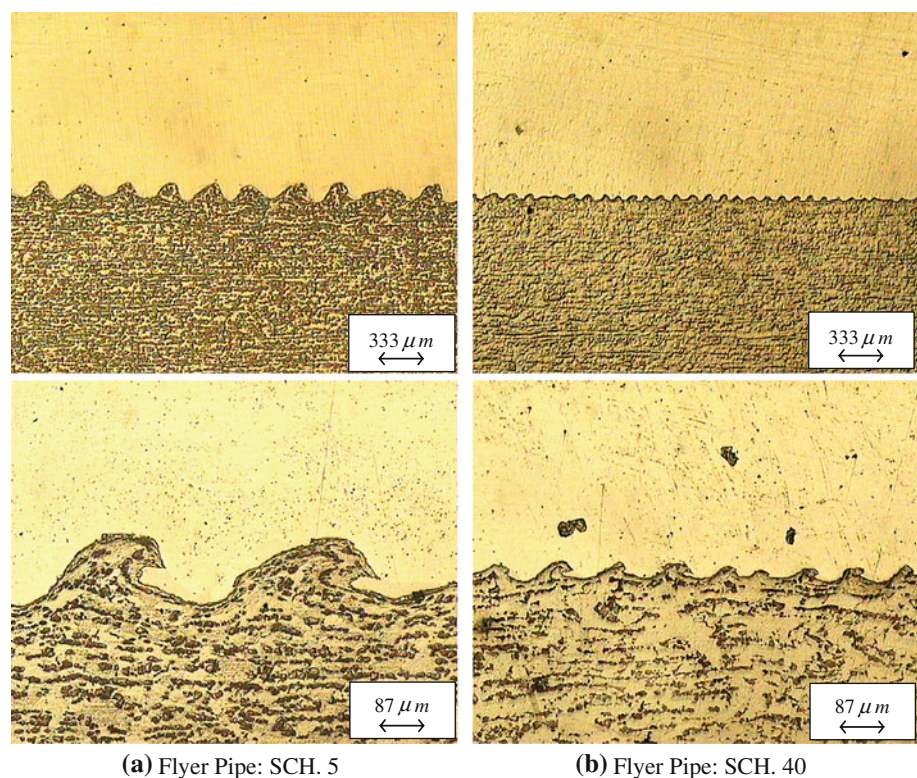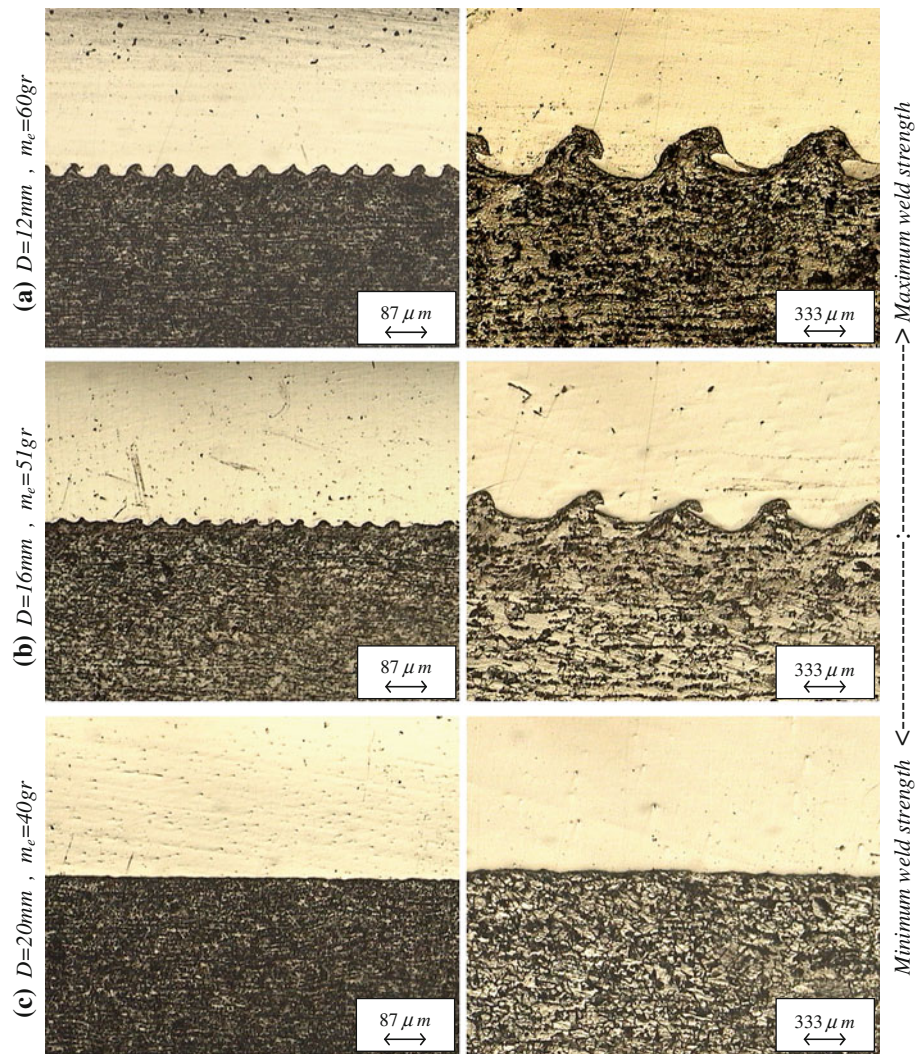
333 μm

333 μm

87 μm

87 μm

(a) Flyer Pipe: SCH. 5   **(b)** Flyer Pipe: SCH. 40

Fig. 12 Turning of the wavy interface into the smooth interface, caused by explosive mass reduction, Flyer: SCH. 5 (*upper layers*: stainless steel, *lower layers*: carbon steel), direction of the detonation front progress: from the *left* to the *right*

$$\beta = 2 \, \sin^{-1}(V_\mathrm{p}/2V_\mathrm{w}) = 9.6°$$

The point with coordinates (5100, 9.6) is located in the wavy region of the weldability window, perfectly (Fig. 4). For the 20 mm diameter insert, which corresponds to the smooth interface (Fig. 12c), collision velocity and its associated angle of collision were obtained as equal to 305 m/s and 3.4°, respectively. Figure 4 further shows that the (5100, 3.4) coordinated point is very close to the transition zone. This shows that the explosive welding parameters for the experiments carried out in this study were suited in the proper locations of the weldability window and also, a good agreement between analytical predictions and experimental results has been achieved.

Charge mass

Yazdani [44] carried out numerous experiments to achieve an applicable relation for calculation of the explosive mass required to join cylinders in the explosive welding process.

His statistical analysis on the experimental results led to the equation below:

$$E_\mathrm{e} = 0.0226 \, \rho_\mathrm{f} \, V_\mathrm{D}^2 \, d_\mathrm{ip}^{1.5} \, t_\mathrm{f}^{0.5} \, L \qquad (13)$$

where, E_e, ρ_f, V_D, d_ip, t_f, and L denote explosive energy, density of flyer pipe, detonation velocity, internal diameter of parent pipe, wall thickness of flyer, and length of the pipes to be joined, respectively. Accuracy and application of this relation were tested for the experiments performed in the present study. Outcomes for the thin and the thick-walled flyer pipes are, respectively, as follows:

(SCH. 5):

$$E_\mathrm{e} = 126.4 \times 10^3 \, J \quad \Rightarrow \quad m_\mathrm{e} = E_\mathrm{e}/E_\mathrm{G} \cong 38 \, \mathrm{gr}$$

(SCH. 40):

$$E_\mathrm{e} = 180.7 \times 10^3 \, J \quad \Rightarrow \quad m_\mathrm{e} = E_\mathrm{e}/E_\mathrm{G} \cong 54 \, \mathrm{gr}$$

where, E_G denotes the Gurney energy of the explosive, which is equal to 3360 J/gr for the TNT used [37]. Comparison between these two masses and the results presented

Fig. 13 The effects of explosive mass reduction on the interface, Flyer: SCH. 40 (*upper layers*: stainless steel, *lower layers*: carbon steel), direction of the detonation front progress: from the *left* to the *right*

(a) $D=4mm$, $m_e=54gr$

87 μm

333 μm

(b) $D=8mm$, $m_e=51gr$

333 μm

333 μm
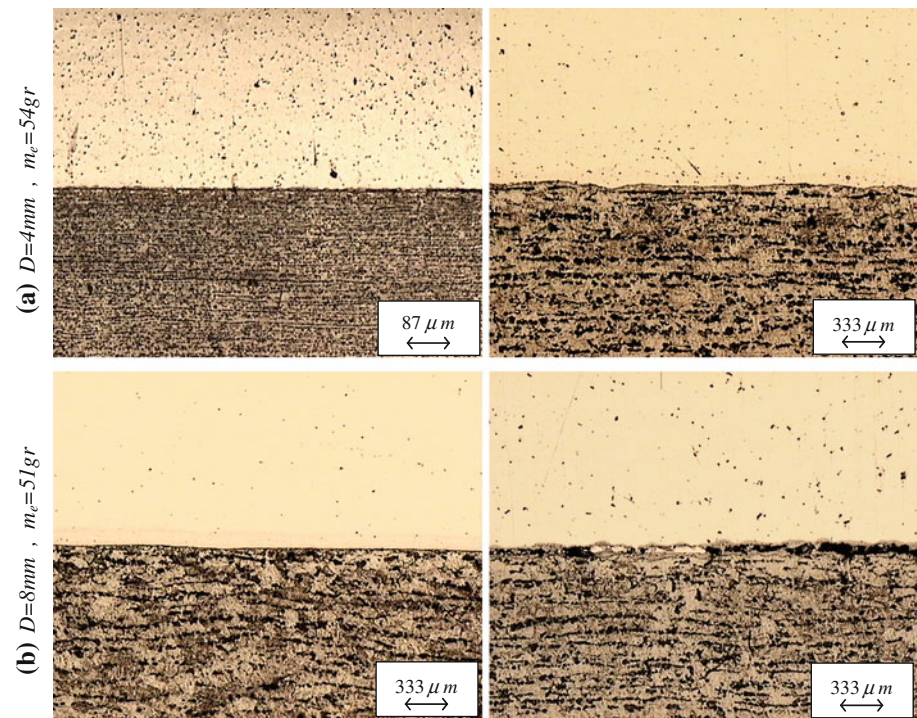
in Figs. 12c and 13a showed that both of the calculated masses were associated to the smooth interface. Therefore, it can be concluded that Eq. 13 calculates the minimum energy required for production of the desired duplex steel pipes.

Conclusion

During the present study, the ability of the explosive welding method in cylindrical geometry appeared. By this method, the internal surface of carbon steel pipes was clad successfully with a thin layer of stainless steel. The weldability domain was defined and used successfully to predict the proper welding parameters for welding. Explosive welding of CK22 carbon steel and AISI 316L stainless steel pipes under different explosive loads were carried out and micro-structural features of interfaces were investigated. The following conclusions can be drawn:

– At low explosive load, the flat interface is produced. The wavy interface is produced at higher explosive loads.
– Wavelength and amplitude of waves are increased with explosive loads.
– Grains near the interface were elongated along the explosive direction due to high localized plastic deformation produced during collision of the metal components.

Finite element calculations of the experiments were carried out. An axisymmetric model of the coaxial pipes was developed. The Johnson-Cook constitutive equation was used for the pipes. Detonation of the charge and expansion of its gaseous products, high rate deformation of the flyer pipe, its collision to the parent pipe, and progress of the collision point along the pipes were covered by the simulation. Numerical analysis allows arbitrary changes in the materials and dimensions without any additional expense, and its outputs can be entered directly into the weldability window, where the location of the associated point determines the quality of the bond with desirable precision. This claim was confirmed properly by the broad experiments performed.

References

1. Raghukandan K (2003) J Mater Proc Technol 139:573
2. Crossland B (1982) Explosive welding of metals and its applications. Clarendon Press, Oxford
3. Akbari Mousavi SAA, Farhadi Sartangi P (2009) Mater Des 30:459
4. Raghukandan K, Rathinasabapathi M, Vaidyanathan PV (1996) J Inst Engrs 77:9
5. Abe A (1999) J Mater Proc Technol 85:162
6. Gerland M, Presles HN, Guin JP, Bertheau D (2000) Mater Sci Eng A 280:311
7. Brasher DG, Butler DJ, Hare AW (1988) In: Murr LE (ed) Shock waves for industrial applications. Noyes Publications, New Jersey

8. Cleland DB (1985) In: Blazynski TZ (ed) Explosive welding, forming and compaction. Applied Science Publishers, London
9. Akbari Mousavi SAA, Burely SJ, Al-Hassnai STS (2005) Int J Impact Eng 31:719
10. Findik F (2011) Mater Des 32:1081
11. Lancaster IF (1984) Metallurgy of welding. Chapman and Hall, London
12. Acarer M, Gulenc B, Findik F (2003) Mater Des 24(8):659
13. Acarer M, Gulenc B, Findik F (2004) J Mater Sci 39(21):6457. doi:10.1023/B:JMSC.0000044883.33007.20
14. Kacar R, Acarer M (2003) Mater Sci Eng A 363:290
15. Kacar R, Acarer M (2004) J Mater Proc Technol 152:91
16. Carlson RJ, Simons CC (1962) BMI-1954. Battelle Memorial Inst, Columbus
17. Segel AWL (1964) A.E.C.L-2209. Atomic Energy of Canada Ltd, Chalk river
18. Willis J, Murdie DC (1962) Sheet metal Ind 39:811
19. Dalrymple DG, Johnson W (1967) Int J Mech Tool Des Res 7:257
20. El-Sobky H (1985) In: Blazynski TZ (ed) Explosive welding, forming and compaction. Applied Science Publishers, London
21. Kahraman N, Gulenc B (2005) J Mater Proc Technol 169:67
22. Kahraman N, Gulenc B, Findik F (2007) Int J Impact Eng 34:1423
23. Nouri MD (2003) PhD Dissertation, Tarbiat Modares University
24. Crossland B (1971) Met Mater 12:401
25. Grignon F, Benson D, Vecchio KS, Meyers MA (2004) Int J Impact Eng 30:333
26. Wittman RH (1973) The influence of collision parameters on the strength and microstructure of an explosion welded aluminum alloy. In: 2nd International symposium on the use of explosive energy in manufacturing, Marianskie Lazni
27. Deribas AA, Simonov VA, Zakcharenco ID (1975) Investigation of the explosive parameters for arbitrary combinations of metal and alloys. 5th International conference on high energy rate fabrications
28. Deribas AA, Kudinov VM, Matveenkov FI, Simonov VA (1967) Fiz goreniya Vzryva 3(1):111
29. Cowan GR, Holtzman AH (1963) J App Phys 34:928
30. Cowan GR, Bergman OR, Holtzman AH (1971) Metall Trans 2:3145
31. Jaramillo D, Szecket A, Inal OT (1987) Mater Sci Eng 91:217
32. Bahrani AS, Crossland B (1964) Inst Mech Eng 179:264
33. Hallquist JO (1998) LS-DYNA Manual. LSTC, Livermore
34. Johnson GR (1993) In: Carleon J (ed) Tactical missile warhead. American Institute of Aeronautics and Astronautics, Washington
35. Karpp RR (1993) In: Carleon J (ed) Tactical missile warhead. American Institute of Aeronautics and Astronautics, Washington
36. Kury JW, Briethaupt RD, Tarver CM (1999) Shock Waves 9:227
37. Cooper PW (1996) Explosive engineering. WILEY-VCH, New York
38. Clutter JK, Belk D (2002) Shock Waves 12:251
39. Darvizeh A, Liaghat GH, Nouri MD (2004) Int J Eng Sci 15:33
40. Murat B, Ken S, Loikkanen MJ (2009) J Aero Eng 22:287
41. Akbari Mousavi SAA, Al-Hassani STS, Atkins AG (2008) Mater Des 29:1334
42. Durgutlu A, Okuyucu H, Gulenc B (2008) Mater Des 29:1480
43. Durgutlu A, Gulenc B, Findik F (2005) Mater Des 26:497
44. Yazdani H (2002) Master's Thesis, Tarbiat Modares University